

# Collective oscillations in driven coagulation

Robin C. Ball,<sup>1,2,\*</sup> Colm Connaughton,<sup>1,3,†</sup> Peter P. Jones,<sup>1,‡</sup> R. Rajesh,<sup>4,§</sup> and Oleg Zaboronski<sup>3,¶</sup>

<sup>1</sup>Centre for Complexity Science, University of Warwick, Gibbet Hill Road, Coventry CV4 7AL, UK

<sup>2</sup>Department of Physics, University of Warwick, Gibbet Hill Road, Coventry CV4 7AL, UK

<sup>3</sup>Mathematics Institute, University of Warwick, Gibbet Hill Road, Coventry CV4 7AL, UK

<sup>4</sup>Institute of Mathematical Sciences, CIT Campus, Taramani, Chennai-600113, India

(Dated: November 20, 2018)

We present a novel form of collective oscillatory behavior in the kinetics of irreversible coagulation with a constant input of monomers and removal of large clusters. For a broad class of collision rates, this system reaches a non-equilibrium stationary state at large times and the cluster size distribution tends to a universal form characterised by a constant flux of mass through the space of cluster sizes. Universality, in this context, means that the stationary state becomes independent of the cut-off as the cut-off grows. This universality is lost, however, if the aggregation rate between large and small clusters increases sufficiently steeply as a function of cluster sizes. We identify a transition to a regime in which the stationary state *vanishes* as the cut-off grows. This non-universal stationary state becomes unstable, however, as the cut-off is increased and undergoes a Hopf bifurcation. After this bifurcation, the stationary kinetics are replaced by persistent and periodic collective oscillations. These oscillations carry pulses of mass through the space of cluster sizes. As a result, the average mass flux remains constant. Furthermore, universality is partially restored in the sense that the scaling of the period and amplitude of oscillation is inherited from the dynamical scaling exponents of the universal regime. The implications of this new type of long-time asymptotic behaviour for other driven non-equilibrium systems are discussed.

PACS numbers: 82.40.Bj,82.40.Ck,83.80.Jx

The statistical dynamics of irreversible coagulation have been studied for almost a century since the pioneering work of Smoluchowski on Brownian coagulation of spherical droplets. See [1] for a modern review. It nevertheless remains an important branch of statistical physics. This is in part due to its status as a paradigm of non-equilibrium kinetics, but primarily due to its connections to variety of important modern problems. We particularly highlight applications in cloud physics [2], surface growth [3] and planetary physics [4]. In these examples, coagulation of clusters is supplemented with a source (or effective source in the case of [4]) of small clusters or “monomers”. Such driven coagulation, in which monomers are supplied to the system at a constant rate, is the main focus of this article. One may expect the kinetics of such a system to become stationary for large times [5] with the loss of clusters due to coagulation compensated by the supply of new clusters provided by the input of monomers. We show below that this intuitive picture is not always correct and demonstrate the possibility of a new and strikingly different long time behavior characterised by time-periodic oscillatory kinetics.

Before we begin, let us introduce a large mass cut-off,  $M$ . Above this size clusters are removed from the system. Physically this could be literal removal as in the case of large droplets preferentially precipitating out of a cloud,

or quenching of reactivity due, for example, to charge accumulation. Our primary motivation for introducing it, however, is theoretical and we shall focus on what happens as  $M \rightarrow \infty$ . The basic quantity of interest is the cluster size distribution denoted by  $N_m(t)$ . It is the average density of clusters of mass  $m$  at time  $t$ . Assuming that the system is statistically homogeneous,  $N_m(t)$  has no spatial dependence. We denote the coagulation rate between clusters (or coagulation “kernel”) by  $K(m_1, m_2)$ . Suppressing the  $t$ -dependence of  $N_m(t)$  for brevity, the mean-field kinetics satisfy Smoluchowski’s equation:

$$\begin{aligned} \partial_t N_m = & \frac{1}{2} \int_1^m dm_1 K(m_1, m - m_1) N_{m_1} N_{m - m_1} \quad (1) \\ & - N_m \int_1^{M - m} dm_1 K(m, m_1) N_{m_1} + J \delta(m - 1) \\ & - D_M [N_m] \end{aligned}$$

where

$$D_M [N_m] = N_m \int_{M - m}^M dm_1 K(m, m_1) N_{m_1} \quad (2)$$

removes clusters larger than  $M$  and  $J$  is the monomer injection rate. We study the family of kernels

$$K(m_1, m_2) = \frac{1}{2} (m_1^\nu m_2^\mu + m_1^\mu m_2^\nu), \quad (3)$$

which includes many of the commonly studied models [1]. Eq. (3) can also capture the asymptotics of most physically relevant kernels. We mostly consider cases for which  $\mu + \nu < 1$ . This avoids complications due to gelation [1].

\* R.C.Ball@warwick.ac.uk

† connaughtonc@gmail.com

‡ P.P.Jones@warwick.ac.uk

§ rrajesh@imsc.res.in

¶ O.V.Zaboronski@warwick.ac.uk

The stationary solution of Eq. (1) without cut-off was found in [6]. It is a power law for large  $m$ :

$$N_m = \sqrt{\frac{J[1 - (\nu - \mu)^2] \cos[\pi(\nu - \mu)/2]}{4\pi}} m^{-\frac{\nu + \mu + 3}{2}}. \quad (4)$$

The exponent  $\frac{\mu + \nu + 3}{2}$  implies a constant flux of mass through the space of sizes,  $m$ . It is a standard example of a non-equilibrium stationary state with a conserved current. From Eq. (4), this stationary state exists only if  $|\nu - \mu| < 1$ , a fact which is true for any scale invariant kernel [7]. One might ask what happens if  $|\nu - \mu| > 1$ ? This can occur in practice. Examples include coagulation of ice clusters in planetary rings [4], gravitational clustering [8] and droplet sedimentation in static fluids [9].

The fact that the constant flux stationary state only exists for a certain class of kernels has long been appreciated in the theory of wave kinetics [10]. There, the constraint  $|\nu - \mu| < 1$  would be interpreted in terms of universality. If one solves the stationary version of Eq. (1) with finite cut-off,  $M$ , and studies the behavior as  $M \rightarrow \infty$  one finds that when  $|\nu - \mu| < 1$ , the leading order terms become independent of  $M$  as  $M \rightarrow \infty$ . The stationary state thus tends to the above universal form found in [6]. If, on the other hand,  $|\nu - \mu| > 1$ , the stationary state is non-universal and retains a dependence on  $M$  as  $M \rightarrow \infty$ . This phenomenon is referred to as *nonlocality* of interaction (in the mass space) in the sense that all masses remain strongly coupled to the largest and smallest masses in the system. By extension, the interactions in the regime  $|\nu - \mu| < 1$  are termed *local* although this is a rather weak form of locality. The presence of a finite cut-off is essential to obtain a stationary state in the nonlocal regime as discussed in [11].

Almost nothing is presently known about the shape of  $N_m$  in the nonlocal regime. We developed an algorithm to compute the exact stationary solution of the discrete version of Eq. (1) with cut-off by converting it into a two-dimensional minimisation problem which can be easily solved numerically for modest values of  $M$ . For details see Appendix A. Some typical results are shown by the symbols in Fig. 1. It is clear that the nonlocal stationary state is not a simple power law. To obtain some analytic understanding, one possible way forward was outlined in [12]. If clusters of size  $m$  grow primarily by interaction with clusters of mass  $m_1 \ll m$ , which is the essential feature of nonlocal interactions, one can Taylor expand the righthand side of Eq. (1) and obtain an almost linear equation for  $N_m(t)$  [12]. The dominant terms in this equation are

$$\frac{\partial N_m}{\partial t} = -D_{\mu+1} \frac{\partial}{\partial m} [m^\nu N_m] - D_\nu N_m, \quad (5)$$

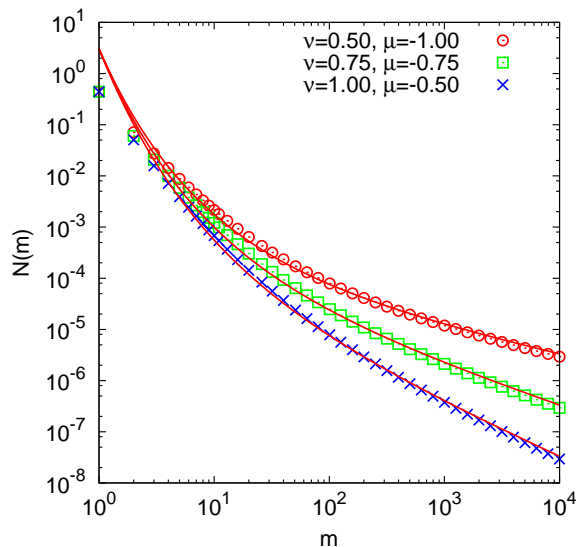


FIG. 1. Comparison of asymptotic approximation, Eq. (6) (solid lines) to the true stationary state of Eq. (1) (symbols) with the kernel given by Eq. (3) for several values of  $\nu$  and  $\mu$  chosen in the nonlocal regime. The cut-off is  $M = 10^4$ .

where the  $t$  dependence of  $N_m$  has been suppressed and

$$D_{\mu+1} = \int_1^{\frac{m}{2}} m_1^{\mu+1} N_{m_1} dm_1 \rightarrow \int_1^M m_1^{\mu+1} N_{m_1} dm_1,$$

$$D_\nu = \int_m^M m_1^\nu N_{m_1} dm_1 \rightarrow \int_1^M m_1^\nu N_{m_1} dm_1.$$

Extension of the limits of integration of these latter integrals to  $M$  and 1 respectively is a further assumption which needs to be justified a-posteriori. The self-consistent calculation detailed in [13] for the case  $\mu = 0$  is easily extended to obtain the following stationary asymptotic solution of Eq. (5) in the limit of large  $M$ :

$$N_m^* \sim \sqrt{2\gamma J \log(M)} M^{-1} M^{m-\gamma} m^{-\nu} \quad (6)$$

where  $\gamma = \nu - \mu - 1$ , adopting the convention that  $\nu > \mu$  in Eq. (3). Detailed derivations of Eqs. (5) and (6) are provided in Appendices B and C. Equation (6) approximates well the true stationary state as indicated by the solid lines in Fig. 1. Note that there are no adjustable parameters. A striking feature of Eq. (6) is that the prefactor of the stationary state *vanishes* as  $M \rightarrow \infty$  reflecting the non-universality of the nonlocal regime. Similar behaviour was observed in the instantaneous gelation regime in [13] although there is no gelation here.

The vanishing of the stationary state in the limit  $M \rightarrow \infty$  poses a conceptual problem since it suggests the removal of the conduit linking the source to the sink. In order to investigate how the conserved mass current is carried in the nonlocal regime, we computed dynamical solutions of Eq. (1) in the nonlocal regime using the numerical algorithm developed in [14]. The results were

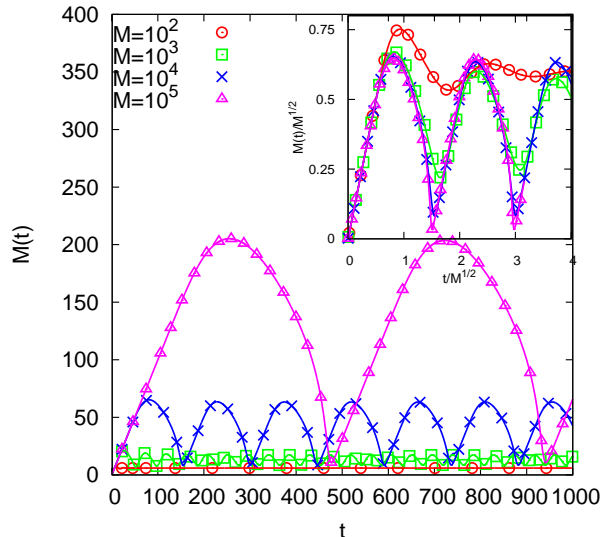


FIG. 2. Main panel: Total mass vs time for different values of  $M$  with  $\nu = -\mu = \frac{3}{2}$ . Inset: Collapse obtained by rescaling the data according to Eqs. (9).

surprising. For small values of  $M$ , the numerical solution converged to the exact stationary state as expected. Once  $M$  exceeded a certain value, however, the numerical solution never reached the stationary state. The typical behaviour of the total mass as a function of time for different values of  $M$  is shown in the main panel of Fig. 2 for the case  $\nu = -\mu = \frac{3}{2}$ . Stationarity is reached only for smaller values of  $M$ . For larger  $M$  we observe collective oscillations which seem to persist indefinitely (we stopped the computation after several hundred periods). The period and amplitude grow with  $M$ .

The intriguing possibility thus arises that the stationary state becomes unstable as  $M$  increases. Our algorithm for computing the stationary state is not dynamical and makes no distinction between stable and unstable fixed points. We therefore input the exact stationary state as an initial condition for the dynamical code and added a small perturbation. The results for the density are shown in the inset of Fig. 3. The perturbation grows to a finite amplitude in a clear indication of instability. A lin-log plot of the amplitude of the successive maxima of the perturbation, as shown in the main panel of Fig. 3, indicates exponential growth, a clear sign of linear instability. We used *Mathematica* to compute the eigenvalue,  $\zeta_{\max}$ , of the linearization of the discrete version of Eq. (1) about the stationary state having maximum real part. This analysis confirmed the instability. The growth rate agrees well with numerics (see main panel of Fig. 3). For fixed  $\nu$  and  $\mu$ , the stationary state undergoes a Hopf bifurcation as  $M$  is increased. The eigenvalue  $\zeta_{\max}$  crosses the imaginary axis at a critical value of  $M$  (see inset of Fig. 4) giving birth to a limit cycle and oscillatory behavior. The structure of the instability as a function of  $\nu$  and  $\mu$  for fixed  $M$  is non-trivial as shown

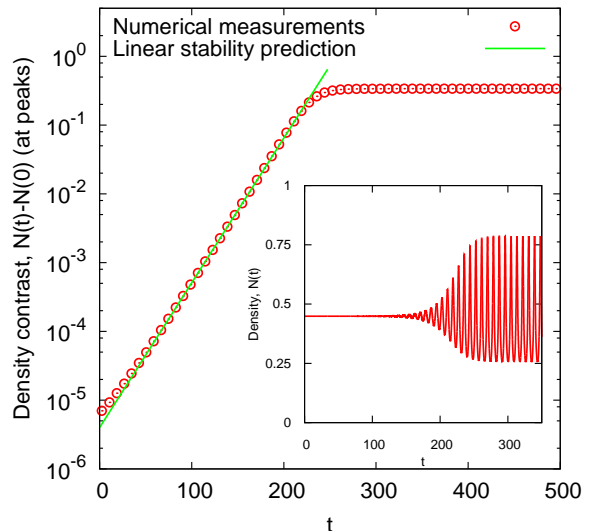


FIG. 3. Numerical evolution of a perturbation of the stationary state for  $\nu = -\mu = \frac{3}{2}$  and  $M = 100$ . Main panel: amplitude of successive maxima of the perturbation (circles). The solid line is the prediction of linear stability analysis. Inset: oscillations of the total density.

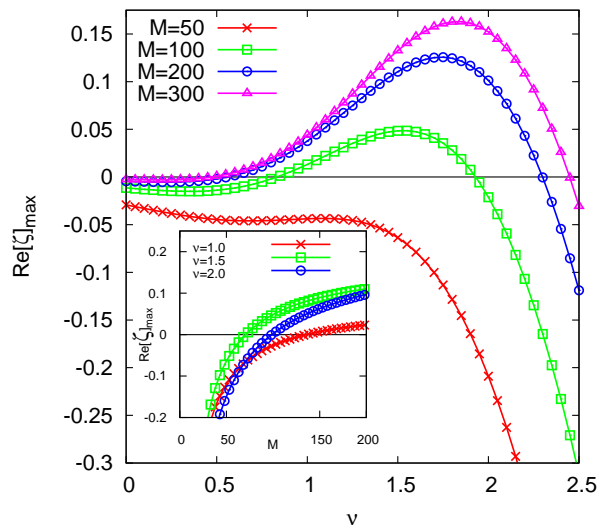


FIG. 4. Main panel:  $\text{Re}[\zeta]_{\max}$  for kernels  $\mu = -\nu$  plotted as a function of  $\nu$  for different values of the cut-off,  $M$ . Inset:  $\text{Re}[\zeta]_{\max}$  as a function of  $M$  for different values of  $\nu$ .

in the main panel of Fig. 4. For fixed  $M$ , the stationary state becomes stable again for sufficiently large values of  $\nu$ , a fact for which we have no intuitive explanation at present. Such limit cycles appearing in mean-field equations can be destroyed by noise[15]. To check the robustness of this phenomenon, we performed Monte-Carlo simulations of the Markus-Lushnikov model (see [16]) with a source and sink of particles. Typical results are shown in Fig. 5. Oscillations are clearly visible which remain coherent in the presence of noise.

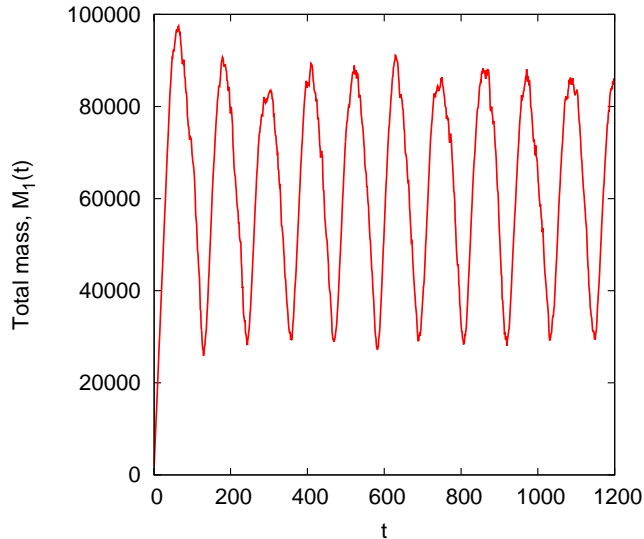


FIG. 5. Total mass vs time in a Monte-Carlo simulation of the Markus-Lushnikov model with a source and sink and kernel given by Eq. (3) with  $\mu = -\nu = -0.95$  and  $M = 300$ .

To understand nonlinear aspects of the instability such as the period and amplitude of nonlinear oscillation we return to Eq. (1). Each period corresponds to a pulse of mass through the space of sizes. A movie provided with the arxiv version of this paper illustrates these pulses. For details of the parameters see Appendix D. Each pulse almost resets the mass of the system to zero as evident from the main panel of Fig. 2. Let us suppose each pulse grows with self-similar size distribution,

$$N_m(t) = s(t)^a F(\xi) \quad \text{with } \xi = \frac{m}{s(t)}, \quad (7)$$

where  $s(t)$  is a typical size and  $a$  is an exponent to be determined. Substituting Eq. (7) into Eq. (1) and balancing dependences on  $t$  requires that  $\dot{s} = s^{\nu+\mu+a+2}$ . Since the mass contained in each pulse grows linearly in time,  $\int_0^M m N_m(t) dm = Jt$ . Substituting Eq. (7) and differentiating gives  $\dot{s} \sim s^{-a-1}$ . Consistency requires

$$a = -\frac{\nu + \mu + 3}{2} \quad s(t) \sim t^{\frac{2}{1-\nu-\mu}}. \quad (8)$$

The period is estimated as the time,  $\tau_M$ , required for the typical mass,  $s(t)$ , to reach  $M$ . The amplitude,  $A_M$ , is estimated as the mass supplied in one period. We thus obtain the following scalings for  $\tau_M$  and  $A_M$  with  $M$ :

$$\tau_M \sim M^{\frac{1-\nu-\mu}{2}} \quad A_M \sim JM^{\frac{1-\nu-\mu}{2}}. \quad (9)$$

These scalings are verified by the data collapse presented in the inset of Fig. 2. Universality is in a sense restored since the earlier universal behavior of Eq.(4) can now be understood as the special case in which  $F(\xi)$  has the special form which cancels  $s(t)$  from  $N_m(t)$  in Eq.(7).

We believe that the phenomena presented here are unlikely to be restricted to coagulation. Many driven dissipative systems with conserved currents must satisfy a locality criterion analogous to the one discussed here [17] and may be candidates for oscillatory behaviour when this criterion is violated. In particular, the kinetic equation for isotropic 3-wave turbulence, which is closely analogous to Eq. (1), becomes nonlocal when  $|\nu - \mu| > 3$  [18]. Furthermore, the oscillatory behaviour discussed in this article may even have been already observed experimentally in measurements of non-equilibrium phase separation of binary mixtures with slowly ramped temperature [19, 20]. In this system, droplets of one phase coagulate inside another during demixing with nucleation providing the source of “monomers” although the coagulation process is not obviously nonlocal in our sense. This nevertheless seems like a potentially fruitful direction for further investigation since the theory presented here makes several testable predictions about the oscillatory kinetics.

## ACKNOWLEDGMENTS

C.C. thanks P. L. Krapivsky for enlightening discussions and encouragement and acknowledges the financial support of the Engineering and Physical Sciences Research Council under grant No. EP/H051295/1.

- 
- [1] F. Leyvraz, Phys. Reports **383**, 95 (Aug. 2003)
  - [2] G. Falkovich, A. Fouxon, and M. G. Stepanov, Nature **419**, 151 (2002)
  - [3] Y. A. Kryukov and J. G. Amar, Phys. Rev. E **83**, 041611 (2011)
  - [4] N. V. Brilliantov, A. S. Bodrova, and P. L. Krapivsky, J. Stat. Mech.: Theor. E, **6**, 11 (2009)
  - [5] W. H. White, J. Colloid Interface Sci. **87**, 204 (1982)
  - [6] H. Hayakawa, J. Phys. A **20**, L801 (1987)
  - [7] C. Connaughton, R. Rajesh, and O. Zaboronski, Phys. Rev. E **69**, 061114 (2004)
  - [8] V. Kontorovich, Physica D **152–153**, 676 (2001)
  - [9] H. Pruppacher and J. Klett, *Microphysics of Clouds and Precipitation*, 2nd ed. (Kluwer Academic Publishers, Dordrecht, The Netherlands, 1997)
  - [10] V. Zakharov, V. Lvov, and G. Falkovich, *Kolmogorov Spectra of Turbulence* (Springer-Verlag, Berlin, 1992)
  - [11] P. L. Krapivsky and C. Connaughton, “Driven Brownian coagulation of polymers,” (2012), j. Chem. Phys. (to appear)
  - [12] P. Horvai, S. V. Nazarenko, and T. H. M. Stein, J. Stat. Phys. **130**, 1177 (2008)

- [13] R. C. Ball, C. Connaughton, T. H. M. Stein, and O. Zaboronski, Phys. Rev. E **84**, 011111 (2011)
- [14] M. Lee, Icarus **143**, 74 (2000) J. Phys. A: Math. Gen. **34**, 10219 (2001)
- [15] M. Mobilia, J. Theor. Bio. **264**, 1 (2010)
- [16] D. J. Aldous, Bernoulli **5**, 3 (Feb. 1999)
- [17] C. Connaughton, R. Rajesh, and O. Zaboronski, Phys. Rev. Lett. **98**, 080601 (2007)
- [18] C. Connaughton, Physica D **238**, 2282 (2009)
- [19] J. Vollmer, G. K. Auernhammer, and D. Vollmer, Phys. Rev. Lett. **98**, 115701 (2007)
- [20] I. J. Benczik and J. Vollmer, Europhys. Lett. **91**, 36003 (2010)

### Appendix A: Algorithm for finding exact stationary solution of the Smoluchowski equation

Consider the discrete form of the stationary Smoluchowski equation:

$$0 = \frac{1}{2} \sum_{m_1=1}^{m-1} K(m_1, m - m_1) N_{m_1} N_{m-m_1} - N_m \sum_{m_1=1}^M K(m, m_1) N_{m_1} + J_{m,1}. \quad (\text{A1})$$

We use the kernel considered in the main text:

$$K(m_1, m_2) = \frac{g}{2} (m_1^\mu m_2^\nu + m_1^\nu m_2^\mu). \quad (\text{A2})$$

Here  $g$  is a constant which can be helpful to keep track of dimensions but which is usually set equal to one. Denote the  $p^{\text{th}}$  moment of the size distribution by

$$\mathcal{M}_p = \sum_{m_1=1}^M m_1^p N_{m_1}.$$

If the moments  $\mathcal{M}_\mu$  and  $\mathcal{M}_\nu$  were known, we could find the solution of (A1) by iteration:

$$N_m = \frac{\mathcal{G}_m + \frac{2J}{g} \delta_{m,1}}{(m^\mu \mathcal{M}_\nu + m^\nu \mathcal{M}_\mu)}, \quad (\text{A3})$$

where  $\mathcal{G}_m$  depends only on the densities of clusters with masses less than  $m$  and is given by

$$\mathcal{G}_m = \frac{1}{2} \sum_{m_1=1}^{m-1} K(m_1, m - m_1) N_{m_1} N_{m-m_1}. \quad (\text{A4})$$

The starting value is obtained by setting  $m = 1$  which gives the monomer density

$$N_1 = \frac{2J/g}{\mathcal{M}_\nu + \mathcal{M}_\mu}. \quad (\text{A5})$$

Given that the solution can be expressed in terms of the two moments  $\mathcal{M}_\mu$  and  $\mathcal{M}_\nu$ , the task is now to self-consistently determine the values of these moments. We can approach this task as a simple two-dimensional optimization problem. Eq. (A3) expresses  $N_m$  as a function of the pair of moments  $N_m(\mathcal{M}_\mu, \mathcal{M}_\nu)$ . We create an objective function,  $\Psi(\mathcal{M}_\mu, \mathcal{M}_\nu)$ , as follows:

$$\Psi(\mathcal{M}_\mu, \mathcal{M}_\nu) = \left[ \mathcal{M}_\mu - \sum_{m=1}^M m^\mu N_m(\mathcal{M}_\mu, \mathcal{M}_\nu) \right]^2 + \left[ \mathcal{M}_\nu - \sum_{m=1}^M m^\nu N_m(\mathcal{M}_\mu, \mathcal{M}_\nu) \right]^2. \quad (\text{A6})$$

The correct values of  $\mathcal{M}_\mu$  and  $\mathcal{M}_\nu$ , which we denote by  $\mathcal{M}_{\mu^*}$  and  $\mathcal{M}_{\nu^*}$ , can be found by minimising  $\Psi(\mathcal{M}_\mu, \mathcal{M}_\nu)$ :

$$(\mathcal{M}_{\mu^*}, \mathcal{M}_{\nu^*}) = \arg \min_{(\mathcal{M}_\mu, \mathcal{M}_\nu)} \Psi(\mathcal{M}_\mu, \mathcal{M}_\nu). \quad (\text{A7})$$

This can be done with any numerical minimization algorithm. We used the Nelder-Mead downhill simplex method. The solution thus obtained is exact to within computational error since no approximations have been made in formulating this procedure.

We remark that the problem does not have to be formulated as an optimization problem. One could treat it as two-dimensional root-finding problem. Furthermore, by summing Eq.(A1), one can derive an independent relationship between  $\mathcal{M}_\mu$  and  $\mathcal{M}_\nu$  (in the limit  $M \rightarrow \infty$ ) which further reduces the problem to a one-dimensional root finding problem. We did experiment with some of these alternatives but settled on the procedure described above as the most numerically stable and reliable approach.

### Appendix B: Derivation of the nonlocal Smoluchowski equation

We assume without loss of generality that  $\nu \geq \mu$ . It is the combination  $\gamma = \nu - \mu - 1$  which determines the locality of the stationary solution of Smoluchowski's equation. The nonlocal case corresponds to  $\gamma > 0$ . We can use the differential approximation outlined in [12] to describe the stationary state in this regime. The first step is to rewrite the Smoluchowski equation in a particular form. Terms describing interactions between a reference mass,  $m$ , and masses less than  $\frac{m}{2}$  are gathered together in one group. Those describing interactions with masses larger than  $\frac{m}{2}$  are gathered together in a second group. Splitting the integrals appropriately and performing some manipula-

tions we obtain:

$$\begin{aligned} \dot{N}_m = & \int_0^{\frac{m}{2}} dm_1 [K(m_1, m-m_1)N_{m-m_1} - K(m_1, m)N_m] N_{m_1} \\ & - N_m \int_{\frac{m}{2}}^M dm_1 K(m, m_1)N_{m_1} + J \delta(m - m_0). \end{aligned} \quad (\text{B1})$$

Consider the first term which accounts for all interactions between clusters of mass  $m$  and those having mass,  $m_1 < \frac{m}{2}$ . If the cascade is nonlocal, these interactions are primarily with those clusters having  $m_1 \ll \frac{m}{2}$ , in which case the integrand is strongly concentrated in the region  $m_1 \ll \frac{m}{2}$ . We can then Taylor expand with respect to  $m_1$  and neglect all terms of  $O(m_1^2)$  or higher to obtain:

$$\begin{aligned} \partial_t N_m = & -\frac{\partial}{\partial m} \left[ \int_0^{\frac{m}{2}} dm_1 K(m, m_1) N_{m_1} N_m \right] \\ & - N_m \int_{\frac{m}{2}}^M dm_1 K(m, m_1) N_{m_1} \\ & + J \delta(m - m_0). \end{aligned} \quad (\text{B2})$$

With the kernel given by Eq. (A2), we get the following equation for the stationary state:

$$\begin{aligned} 0 = & -\frac{d}{dm} [\mathcal{M}_{\nu+1}^< m^\mu N_m] - \frac{d}{dm} [\mathcal{M}_{\mu+1}^< m^\nu N_m] \\ & - \mathcal{M}_\nu^> m^\mu N_m - \mathcal{M}_\mu^> m^\nu N_m + \frac{2J}{g} \delta(m - m_0), \end{aligned} \quad (\text{B3})$$

where  $\mathcal{M}_p^>$  and  $\mathcal{M}_p^<$  denote the upper and lower partial moments:

$$\mathcal{M}_p^< = \int_{m_0}^{\frac{m}{2}} dm_1 m_1^p N_{m_1} \quad (\text{B4})$$

$$\mathcal{M}_p^> = \int_{\frac{m}{2}}^M dm_1 m_1^p N_{m_1}. \quad (\text{B5})$$

The dominant terms in this equation when  $m \gg m_0$  will turn out to be

$$\begin{aligned} 0 = & -\frac{d}{dm} [\mathcal{M}_{\mu+1}^< m^\nu N_m] - \mathcal{M}_\nu^> m^\mu N_m \\ & + \frac{2J}{g} \delta(m - m_0). \end{aligned}$$

This statement will have to be justified a-posteriori. In order to make further progress let us assume that the error made by extending the upper and lower limits of integration in the partial moments  $\mathcal{M}_{\mu+1}^<$  and  $\mathcal{M}_\nu^>$  to  $M$  and  $m_0$  respectively is small. This will also have to be justified a-posteriori. The resulting equation is:

$$\begin{aligned} 0 = & -\frac{d}{dm} [\mathcal{M}_{\mu+1}^< m^\nu N_m] - \mathcal{M}_\nu^> m^\mu N_m \\ & + \frac{2J}{g} \delta(m - m_0). \end{aligned} \quad (\text{B6})$$

This is Eq.(5) in the main text.

### Appendix C: Asymptotic solution of nonlocal Smoluchowski equation

Eq.(B6) is a linear equation and can be readily integrated to give

$$N_m = C e^{\frac{\beta}{\gamma} m^{-\gamma}} m^{-\nu} \quad (\text{C1})$$

where  $\beta$  is a ratio of moments

$$\beta = \frac{\mathcal{M}_\nu}{\mathcal{M}_{\mu+1}} \quad (\text{C2})$$

and  $C$  is a constant of integration. The non-trivial aspect of the problem is that the moments  $\mathcal{M}_\nu$  and  $\mathcal{M}_{\mu+1}$  must be determined self-consistently from this solution. This cannot be done analytically but an asymptotic solution for large cutoff,  $M$ , can be found which we now describe. A general moment of order  $\alpha$  is

$$\begin{aligned} \mathcal{M}_\alpha = & C \int_{m_0}^M dm m^{\alpha-\nu} e^{\frac{\beta}{\gamma} m^{-\gamma}} \\ = & \frac{C}{\beta} \left( \frac{\beta}{\gamma} \right)^{\zeta_\alpha+1} \int_{\frac{\beta}{\gamma} M^{-\gamma}}^{\frac{\beta}{\gamma} m_0^{-\gamma}} t^{-\zeta_\alpha-1} e^t dt \end{aligned} \quad (\text{C3})$$

where we have introduced the shorthand notation  $\zeta_\alpha$  for the combination

$$\zeta_\alpha = \frac{1 - \nu + \alpha}{\gamma}.$$

Since  $\mu > \nu + 1$  in the nonlocal regime, we would expect the moment  $\mathcal{M}_\nu$  to grow faster than  $\mathcal{M}_{\mu+1}$  as the cutoff,  $M$ , is increased. We therefore expect  $\beta$  to grow as  $M$  grows. Let us suppose that it does not grow faster than  $M^\gamma$ . If this is the case then the upper limit of the integral in Eq.(C3) tends to infinity as  $M$  grows while the lower limit tends to zero. We are therefore interested in the behaviour of the integral

$$I(\epsilon, \Lambda, \zeta_\alpha) \int_\epsilon^\Lambda t^{-\zeta_\alpha-1} e^t dt$$

as  $\epsilon \rightarrow 0$  and  $\Lambda \rightarrow \infty$ . This integral clearly diverges at its upper limit regardless of the value of  $\zeta_\alpha$ . The leading order behaviour as the upper limit grows is

$$I(\epsilon, \Lambda, \zeta_\alpha) \sim \Lambda^{-\zeta_\alpha-1} e^\Lambda \quad \text{as } \Lambda \rightarrow \infty. \quad (\text{C4})$$

It is divergent at its lower limit if  $\zeta_\alpha > 0$ . The leading order behaviour as the lower limit goes to zero is

$$I(\epsilon, \Lambda, \zeta_\alpha) \sim \frac{1}{\zeta_\alpha} \epsilon^{-\zeta_\alpha} \quad \text{as } \epsilon \rightarrow 0. \quad (\text{C5})$$

The moments of immediate interest correspond to  $\alpha = \nu$  and  $\alpha = \mu + 1$  which give values for  $\zeta_\alpha$  of  $\frac{1}{\gamma}$  and  $\frac{1-\gamma}{\gamma}$  respectively. For  $\alpha = \nu$ , we always get a divergence at the lower limit. For  $\alpha = \mu + 1$  we get a divergence at the lower limit for  $\gamma$  in the range  $0 < \gamma < 1$ . With this knowledge

in mind, our task is now to substitute Eq.(C3) into the consistency condition, Eq.(C2) and attempt to balance the divergences as  $M$  (and thus  $\beta$ ) tends to infinity. One solution is to balance the divergence coming from the lower limit of  $\mathcal{M}_{\mu+1}$  with the one coming from the upper limit of  $\mathcal{M}_\nu$ . This gives, after some work

$$\beta \sim \gamma m_0^\gamma \ln \frac{M}{m_0} \quad \text{as } M \rightarrow \infty, \quad (\text{C6})$$

which is consistent with our assumption that  $\beta$  should grow with  $M$  but slower than  $M^\gamma$ . We can now substitute this value for  $\beta$  into Eq.(C3) and obtain the leading order behaviour of  $\mathcal{M}_\nu$  and  $\mathcal{M}_{\mu+1}$ . We find that  $\mathcal{M}_\nu$  is dominated by its upper limit and grows as

$$\mathcal{M}_\nu \sim C m_0 \left( \frac{M}{m_0} \right) \quad \text{as } M \rightarrow \infty. \quad (\text{C7})$$

On the other hand  $\mathcal{M}_{\mu+1}$  is dominated by its lower limit and grows as

$$\mathcal{M}_{\mu+1} \sim C m_0^{1-\gamma} \left( \frac{M}{m_0} \right) \ln \left( \frac{M}{m_0} \right)^{-1} \quad \text{as } M \rightarrow \infty. \quad (\text{C8})$$

These estimates justify our replacement of the partial moments with full moments in the derivation of Eq.(B6).

It remains to find the constant  $C$ . This can be done by requiring that the total mass flux leaving the system is equal to the input flux,  $J$ :

$$J = \int_{m_0}^M dm m \int_{M-m}^M dm_1 K(m, m_1) N_m N_{m_1}. \quad (\text{C9})$$

Substituting the kernel Eq.(A2) into this gives two terms:

$$\begin{aligned} \frac{2J}{g} &= \int_{m_0}^M dm m^{\mu+1} N_m \int_{M-m}^M dm_1 m_1^\nu N_{m_1} \\ &+ \int_{m_0}^M dm m^{\nu+1} N_m \int_{M-m}^M dm_1 m_1^\mu N_{m_1}. \end{aligned}$$

With some further analysis one finds that the second term is much smaller than the first term as  $M$  grows. Extending the regions of integration of the partial moments as before we obtain the estimate:

$$\frac{2J}{g} \sim \mathcal{M}_{\mu+1} \mathcal{M}_\nu \quad \text{as } M \rightarrow \infty.$$

Using Eqs. (C7) and (C8) we obtain

$$C = \frac{m_0}{M} \sqrt{\frac{2\gamma J}{g} m_0^{\gamma-2} \ln \left( \frac{M}{m_0} \right)}. \quad (\text{C10})$$

Putting this together with Eqs. (C1) and (C6) we finally obtain:

$$\begin{aligned} N_m^* &\sim \sqrt{\frac{2\gamma J}{g} m_0^{-\frac{\nu+\mu+3}{2}}} \sqrt{\ln \left( \frac{M}{m_0} \right)} \left( \frac{M}{m_0} \right)^{-1} \\ &\times \left( \frac{M}{m_0} \right)^{\left( \frac{m}{m_0} \right)^{-\gamma}} \left( \frac{m}{m_0} \right)^{-\nu}. \end{aligned} \quad (\text{C11})$$

The explicit dependence on the monomer mass,  $m_0$  (which we usually take equal to 1) has been retained in order to make the dimensional correctness of the formula clear. Setting  $m_0 = 1$  gives Eq. (6) in the main text.

#### Appendix D: Comment on the accompanying movie

The movie accompanying the arxiv version of this paper shows the time evolution of the density contrast,  $N(m, t)/N^*(m)$ , relative to the stationary state as a function of cluster size,  $m$ , in the oscillatory regime. This quantity would be 1 if the stationary state were stable. Both axes are linear. The movie was generated by solving the discrete Smoluchowski equation (without coarsegraining) with  $\nu = -\mu = \frac{3}{2}$ , a monomer input rate of  $J = 1$  and a cut-off of  $M = 100$ .